J. Am. Chem. Soc. **1979**, *101*, 6783.

Davidova, N.; Peshev, N.; Shopov, D. Some Aspects of the Bifunctional Action of Nickel-Zeolite Catalysts in the Conversion of Toluene. *J. Catal.* **1979**, *58*, 198.

Feng, C.; Stewart, W. E. Practical Models for Isothermal Diffusion and Flow of Gases in Porous Solids. *Ind. Eng. Chem. Fundam.* **1973**, *12*, 143.

Forni, L.; Viscardi, C. F. Sorption-Diffusion in Molecular Sieves. II. Aromatics in Y and ZSM-5 Zeolites. *J. Catal.* **1986**, *97*, 480.

Froment, G. F.; Bischoff, K. B. *Chemical Reactor Analysis and Design*; Wiley: New York, 1979; pp 143-197.

Fu, C.-C.; Ramesh, M. S. P.; Haynes, H. W., Jr. Analysis of Gas Chromatography Pulse Dispersion Data for the System n-Butane/Zeolite NaY. *AIChE J.* **1986**, *32*, 1848.

Gnep, N. S.; Guisnet, M. Toluene Disproportionation over Mordenites. II. Kinetic Study. *Appl. Catal.* **1981**, *1*, 329.

Haag, W. C.; Lago, R. M.; Weisz, P. B. Transport and Reactivity of Hydrocarbon Molecules in a Shape Selective Zeolite. *Discuss Faraday Soc.* **1982**, *72*, 319.

Hopper, J. R.; Voorhies, A., Jr. Hydroisomerization of Cyclohexane and n-Pentane over Series of Mordenite Catalysts of Varying Silica-Alumina Ratio. *Ind. Eng. Chem. Prod. Res. Dev.* **1972**, *11*, 294.

Hyun, S. H.; Danner, R. P. Adsorption Equilibrium Constants and Intraparticle Diffusivities in Molecular Sieves by Tracer-Pulse Chromatography. *AIChE J.* **1985**, *31*, 1977.

Izumi, Y.; Shiba, T. Characterization of the Alumina-Boria Catalyst. *Bull. Chem. Soc. Jpn.* **1964**, *37*, 1797.

Jacobs, P. A.; Leeman, H. E.; Uytterhoeven, J. B. Active Sites in Zeolites. II. Cumene Cracking and Toluene Disproportionation Activity of Stabilized Faujasite Structures. *J. Catal.* **1974**, *33*, 31.

Kaeding, W. W. Selective Production of Para-Xylene. U.S. Patent 4067920, 1978.

Kaeding, W. W.; Young, L. B. Selective Production of Para-Xylene. U.S. Patent 4034053, 1977.

Kaeding, W. W.; Chu, C.; Young, L. B.; Butter, S. A. Shape-Selective Reactions with Zeolite Catalysts. II. Selective Disproportionation of Toluene to Produce Benzene and p-Xylene. *J. Catal.* **1981**, *69*, 392.

Karger, J.; Ruthven, D. M. On the Comparison Between Macroscopic and N.M.R. Measurements of Intracrystalline Diffusion in Zeolites. *Zeolites* **1989**, *9*, 267.

Karger, J.; Bulow, M.; Struve, P.; Kocirik, M.; Zikanova, A. Intercrystalline Molecular Transport in Zeolites Studied by Uptake Experiments and by Nuclear Magnetic Resonance Pulsed Field Gradient Techniques. *J. Chem. Soc., Faraday Trans. 1* **1978**, *74*, 1210.

Karger, J.; Pfeifer, H.; Rauscher, M.; Walter, T. Self-Diffusion of n-Paraffins in NaX Zeolite. *J. Chem. Soc., Faraday Trans. 1* **1980**, *76*, 717.

Lee, J. C.; Luss, D. *Ind. Eng. Chem. Fundam.* **1969**, *8*, 597.

Matsumoto, H.; Morita, Y. Activity of Synthetic Zeolite Catalysts in the Disproportionation Reaction of Toluene. *J. Jpn. Pet. Inst.* **1967**, *8*, 572.

Meier, W. M.; Olson, D. H. *Atlas of Zeolite Structure Types*; Structure Commission of the International Zeolite Association: New York, 1978.

Meshram, N. R. Selective Toluene Disproportionation Over ZSM-5 Zeolites. *J. Chem. Technol. Biotechnol.* **1987**, *37*, 111.

Nayak, V. S.; Riekert, L. Catalytic Activity and Product Distribution in the Disproportionation of Toluene on Different Preparations of Pentasil Zeolite Catalyst. *Appl. Catal.* **1986**, *23*, 403.

Olson, D. H.; Haag, W. O. Structure-Selectivity Relationship in Xylene Isomerization and Selective Toluene Disproportionation. *Am. Chem. Soc., Symp. Ser.* **1984**, *248*, 275.

Poutsma, M. L. Mechanistic Considerations of Hydrocarbon Transformations Catalyzed by Zeolites. In *Zeolite Chemistry and Catalysis*; Rabo, J. A., Ed.; American Chemical Society: Washington, DC, 1976; p 437.

Pukanic, G. W.; Massoth, F. E. Kinetics of Mesitylene Isomerization and Disproportionation over Silica-Alumina Catalyst. *J. Catal.* **1973**, *28*, 308.

Ragaini, V.; Fois, R.; LeVan Mao, R.; Cattania, M. G. A Simplified Calculation Method to Evaluate Intraparticle Diffusivity from Sorption Kinetic Measurements. Application of the Diffusion of Xylenes in 13X and ZSM Zeolites. *Can. J. Chem. Eng.* **1984**, *62*, 706.

Reid, R. C.; Prausnitz, J. M.; Sherwood, T. K. *The Properties of Gases and Liquids*, 3rd ed.; McGraw-Hill: New York, 1977.

Satterfield, C. N. *Heterogeneous Catalysis in Practice*; McGraw-Hill: New York, 1980; pp 344-348.

Satterfield, C. N.; Katzer, J. R.; Vieth, W. R. Desorption and Counterdiffusion Behavior of Benzene and Cumene in H-Mordenite. *Ind. Eng. Chem. Fundam.* **1971**, *10*, 478.

Schulz-Ekloff, G.; Jaeger, N. I.; Vladov, C.; Petrov, L. Effects of Carrier Gases in the Toluene Disproportionation on H-ZSM-5 Zeolite. *Appl. Catal.* **1987**, *33*, 73.

Streitwieser, A., Jr.; Reif, L. Mechanisms of Transalkylation of Ethylbenzene. *J. Am. Chem. Soc.* **1960**, *82*, 5003.

Weisz, P. B. Molecular Shape-Selective Catalysis. *Pure Appl. Chem.* **1980**, *52*, 2091.

Wu, J.-C.; Leu, L.-J. Toluene Disproportionation and Transalkylation Reaction over Mordenite Zeolite Catalysts. *Appl. Catal.* **1983**, *7*, 283.

Wu, P.-D.; Debebe, A.; Ma, Y. H. Adsorption and Diffusion of C_6 and C_8 Hydrocarbons in Silicalite. *Zeolites* **1983**, *3*, 118.

Yashima, T.; Moslehi, H.; Hara, N. Disproportionation of Toluene on Synthetic Mordenites. *Bull. Jpn. Pet. Inst.* **1970**, *12*, 106.

Received for review February 21, 1989
Revised manuscript received October 13, 1989
Accepted January 30, 1990

Effect of Catalysts on the Kinetics of the Reduction of Barite by Carbon[†]

Satish B. Jagtap, Anita R. Pande, and Ashok N. Gokarn*
Chemical Engineering Division, National Chemical Laboratory, Pune 411 008, India

Reduction of high-grade barite powder with particles of active charcoal has been studied both in the absence and presence of catalysts. Catalysts that are known to enhance Boudouard reaction bring about corresponding improvements in the reduction rate of barite also. The conversion-time data have been analyzed by using a modified volume reaction model, and the effect of catalysts on kinetic parameters has been elucidated.

Reduction of barite by solid carbon is an important step for the recovery of barium chemicals from barite. In this so-called "black ash process" (McKetta, 1977), the reduction of barite is carried out in a rotary kiln or in a fluidized bed at a high temperature of the order of 1100-1200 °C in the presence of reducing agents, mostly carbon. In the course of the reduction, the main reducing agent is carbon monoxide, which in turn is generated in situ by the reduction of carbon dioxide by carbon. The reactivity of coal is generally correlated by its reactivity with CO_2 to generate

---

[†] NCL Communication 4558.

CO. By using highly reactive coal/coke, it is possible to bring down the reduction temperature, resulting in greater energy savings. Most of the coal/coke used for the reduction process is less reactive, and the reactivity can be increased to a great extent by incorporating inorganic salts belonging to alkali and alkaline-earth metal groups as well as transition-metal groups (McKee, 1981). The reaction of CO_2 with coal (which is incorporated with these inorganic salts) is enhanced considerably and thus imparts a high reactivity.

Earlier studies on the kinetics of reduction of barite by carbon have been very limited. Only a few Russian scientists (Shushunov et al., 1954; Pechkovski and Ketov, 1960; Ravdel and Novikova, 1963) have carried out mechanistic studies of the reduction of barite by carbon. All are unanimous of the opinion that the initial reduction of barite with carbon takes place according to

$$BaSO_4 + 4C \rightarrow BaS + 4CO \tag{1}$$

where both barite and carbon are in contact. The CO generated diffuses and reacts with barite, which is not in contact with carbon, according to

$$BaSO_4 + 4CO \rightarrow BaS + 4CO_2 \tag{2}$$

This CO_2 diffuses back into carbon to generate more CO according to the Boudouard reaction:

$$C + CO_2 \rightarrow 2CO \tag{3}$$

Thus, in the solid-state reduction of barite, CO is a gaseous intermediate.

The only kinetic study reported on the reduction of barite by carbon is that of Lozhkin et al. (1974). They have investigated the kinetic mechanism of pure $BaSO_4$ and barite ore. In both cases, they have noticed that the reduction took place according to the mechanism (through gaseous intermediate) referred to above. They also agree with the findings of Ravdel and Novikova (1963) that the rate of reduction eq 2 is quite higher than that of the Boudouard reaction, eq 3. Thus, the overall rate is controlled by the progress of the C + CO_2 reaction, which is slower. By monitoring the conversion of barite to barium sulfide, they have proposed that the overall reduction of barite is controlled by reaction kinetics, in the low-temperature range (900–1020 °C) with an activation energy of 54.1 kcal/mol. The kinetic control model for this reaction, which is derived on the basis of the popular shrinking core mechanism of Levenspiel (1962), is

$$k\tau = 1 - (1 - x)^{1/3} \tag{4}$$

where k is the rate constant, τ is the time, and x is the fractional conversion of barite. Similarly in the high-temperature range (1140–1200 °C), they have shown that the experimental data of the reduction of barite with coke could be modeled according to the shrinking core mechanism of diffusion control as proposed by Wen (1968), in which the effective diffusivity is based on the surface area of the unreacted core. The equation is

$$k^2\tau = [1 - (1 - x)^{1/3}]^2 \tag{5}$$

with an activation energy of 17.0 kcal/mol.

Very recently, Pelovski et al. (1987) studied the reduction of barium sulfate by carbon in the presence of inorganic salts like sodium carbonate, sodium chloride, and calcium chloride and observed that these additives act as promoters for the reduction process. It is not known whether these salts were added directly into the reduction mass or impregnated in the matrix of either of the reactants. In the temperature range 786–871 °C studied for the reduction of barite, they obtained an activation energy of 59.1 kcal/mol.

Table I. Analysis of Active Charcoal and Barite

active charcoal		barite	
component		component	
fixed carbon	98.0 wt %	$BaSO_4$	98.0
ash	1.5 wt %	SiO_2	0.40
volatile matter	nil	Al_2O_3	0.05
moisture	0.5 wt %	Fe_2O_3	0.04
initial surface area	600 m^2/g	porosity	nonporous particles
initial av porosity	44%		

Thus, from the earlier study on barite reduction, it is clear that the reduction is a two-step process as described by eqs 2 and 3, and the second step, viz. Boudouard reaction represented by eq 3, is rate controlling. This is a typical example of a solid–solid reaction ($BaSO_4$–C) proceeding through a gaseous intermediate (CO here) as described by Sohn and Szekely (1973) and Wynnyckyj and Rankin (1988). Hence, our objective here to increase the reduction rate of barite by carbon is justified if we are able to increase the reactivity of carbon (thereby enhancing the Boudouard reaction). Since the main reducing agent is CO, the progress of barite reduction could either be followed by the rate of carbon consumption or analysis of the reaction product, viz. barium sulfide, at various time intervals. Since reduction of barite involves knocking out oxygen from barium sulfate, step by step, it is easier to follow the overall kinetics by analyzing BaS formed at various time intervals.

It has been the aim of the present investigation to study the reaction mechanism of barite reduction by carbon and propose a kinetic model, both in the presence and absence of catalyst. We have used fine powder of barite (particle size of 0.044 mm) to overcome the diffusion limitation and ensure that the reaction is carried out in the kinetic-controlled region only (Doraiswamy and Sharma, 1984).

Experimental Section

The experiments were carried out as small-scale batch experiments of a boat-in-tube setup. For this, commercial grade samples of barites were supplied by Hindustan Mineral Products Co., Bombay, India. For the study of the reduction by carbon, activated charcoal was used. The chemical analysis and physical properties of barite and activated charcoal are given in Table I. For the most part, in the present study, fine-sized barite (−250 mesh) and coarse-sized carbon (−30 to 60 mesh) were used. The combination of particle sizes of carbon and barite is comparable with that used in industrial practice. Reagent grade Na_2CO_3 and $Fe(NO_3)_3$ were used as the catalyst.

Sample Preparation. Barite and active charcoal powders were separately weighed and mixed thoroughly. The active charcoal used in the catalytic runs was impregnated with different catalyst solutions. Due to the high initial porosity and surface area of the active charcoal, a uniform catalyst distribution could be achieved by incipient wetting of active charcoal in the catalytic solution for 24 h. The impregnated active charcoal was dried at 120 °C and stored in a closed container.

In all cases, a stoichiometric composition of reacting solids (i.e., $BaSO_4$ + 4C) was used.

Procedure. The experimental setup consisted of a 50-mm-diameter tubular furnace (Harrop Inc. make) with a 25-mm-diameter tubular silica reactor. A weighed quantity of charge (2.33 g of barite and 0.48 g of a stoichiometric amount of active charcoal) was mixed thoroughly and placed in a silica boat (11-mm diameter, 50 mm long). The sample boat was first introduced in the less hot

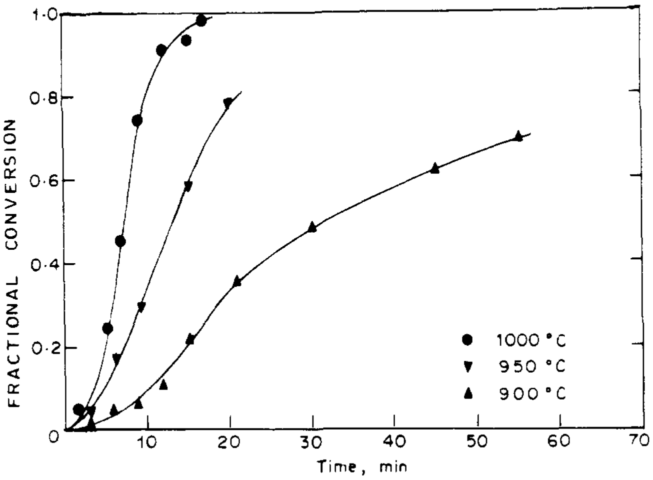

Figure 1. Conversion–time plots for the reduction of barite by active charcoal (noncatalytic).

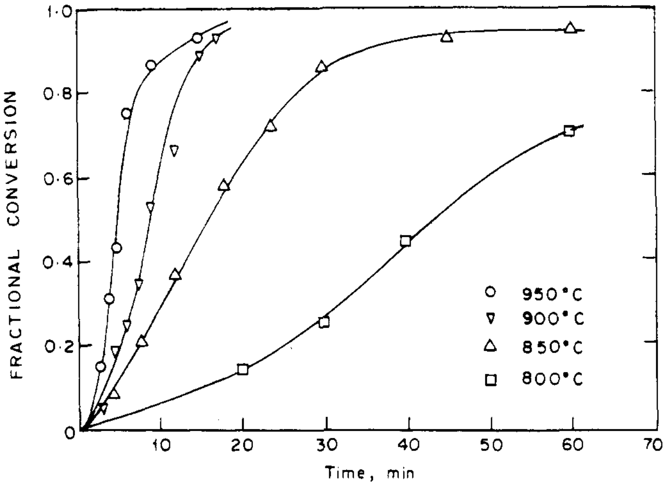

Figure 2. Conversion–time plots for the reduction of barite by active charcoal with 5% Na_2CO_3.

zone of the reactor. After 5 min, the sample boat was pushed into the central hot zone of the reactor that was maintained at the desired temperature. This procedure helped in reducing the time required for the sample boat to attain the reaction temperature. Also the sample size was found to be optimum considering the measurable conversion for kinetic studies and the minimum time required for attainment of the reaction temperature. The reactor system was made oxygen free with a slow stream of ultrapure nitrogen at a flow rate of 1 mL/s, before and during the run. Zero time was counted when the boat containing the sample was pushed into the reactor that was maintained at the desired temperature. After a stipulated time period, the reaction could be stopped by sliding the boat from the central hot zone to the cool outer zone of the tube. The cooled sample was weighed and analyzed for percentage barium sulfide by the iodometry method (Snell and Hilton, 1984) for each run. The entire experimental procedure was found to give satisfactory reproducible results.

Process Variables. The process variables were as follows: (A) temperature, reduction temperature of 800–1000 °C; (B) catalyst used, Na_2CO_3 or $Fe(NO_3)_3$ (5 % each based on weight of active charcoal); (C) height of the bed, approximately 5 mm in all the runs.

Results and Discussion

Nature of the Conversion–Time Plots. Conversion–time plots shwon in Figures 1–3 refer to the reduction of barite to barium sulfide by active charcoal under noncatalytic, Na-catalyzed, and Fe-catalyzed conditions, respectively. All the plots are identical in nature and are characterized by sigmoidal behavior and the typically initial slow reaction, followed by accelerated rate and ending with decelaration. This kind of behavior is generally observed in the reactions involving decomposition of solids, in the dehydration of hydrated salts, and most commonly in the gasification of coal chars, where the cause for sigmoidal conversion–time data is the nature of pore development and corresponding structural changes in the reacting solid (Kasaoka et al., 1982). In the present investigation, the observed sigmoidal behavior can be attributed to the Boudouard reaction ($C + CO_2$) involved in the total reaction system. Here the amount of CO generated (i.e., gaseous intermediate) is directly proportional to the rate of the $CO_2 + C$ reaction, and reduction of barite is directly linked to the amount of CO generated; thus, the rate of barite reduction (monitored by the chemical analysis method) should be a mirror reflection of the Boudouard reaction. This fact is evident from the observed linear relationship between the fractional conversion of barite to barium sulfide and the weight loss of the reaction sample during experiments. Thus, it can be stated that in the present reaction system there is one-to-one correspondence between the gasification step (Boudouard reaction) and the barite reduction step. Also, in a recent study of the reduction of sodium sulfate by carbon, Cameron and Grace (1983) have experimentally proved that the kinetics of the reduction of Na_2SO_4 is directly related to structural changes taking place in the carbon.

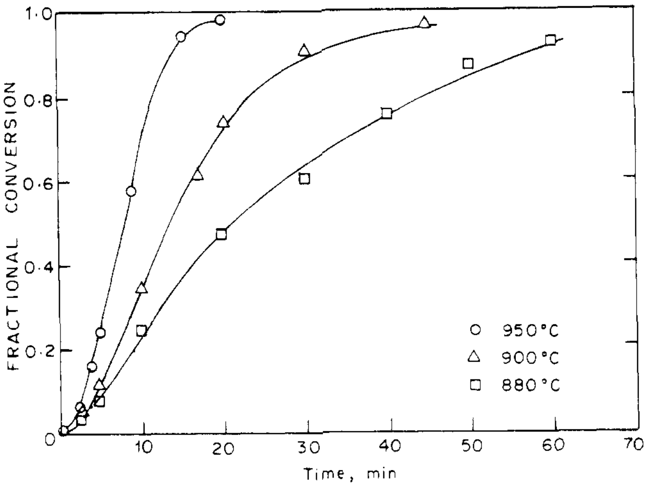

Figure 3. Conversion–time plots for the reduction of barite by active charcoal with 5% $Fe(NO_3)_3$.

Application of the Modified Volume Reaction Model to Kinetic Data. To obtain the kinetic parameters and thereby to compare the effect of catalysis, a modified volume reaction (MVR) model, developed by Kasaoka et al. (1983), has been applied to the conversion–time data from Figures 1–3. This significantly simple mathematical model depicts structural changes taking place in the matrix of carbon during gasification and also accounts for sigmoidal behavior of conversion–time data of various carbons (Kasaoka et al., 1985). Since the reduction of barite by carbons falls in the kinetic-controlled region and goes through a gaseous intermediate (via CO), application of this model is justified. The model equation proposed by Kasaoka and Sakata (1984) is

$$x = 1 - \exp(-a\theta^b) \qquad (6)$$

where x is the fractional conversion, θ is the time in seconds, and a and b are constant parameters. Model pa-

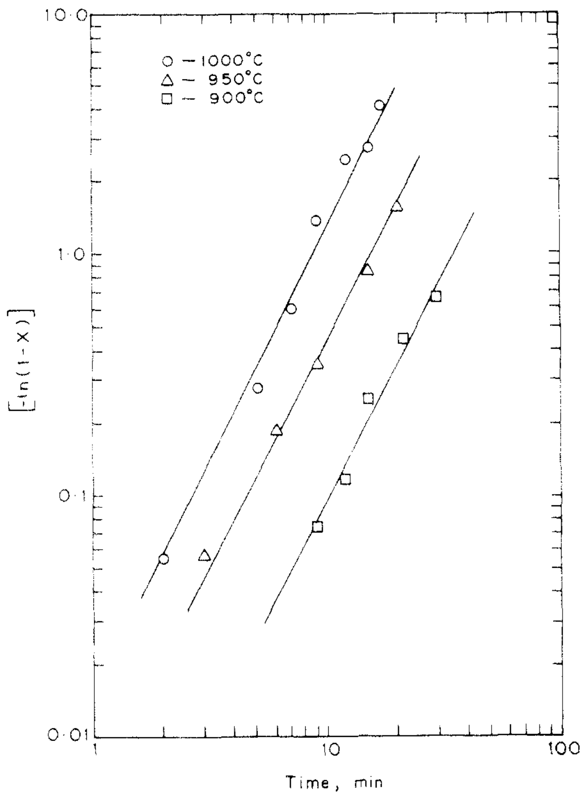

Figure 4. Application of the MVR model to the reduction of barite by active charcoal (noncatalytic).

rameter a is related to the kinetic rate constant of the reaction and is temperature dependent. Parameter b is related to the physical changes occurring in the carbon matrix. Parameter b is very important since its value determines the reaction characteristics. Thus, for $b = 1$, the reaction follows homogeneous first-order kinetics; for $b > 1$, a sigmoidal behavior is guaranteed. (In the present study, the value of b varied between 1.1 and 2.4.) The model given by eq 6 is a general one and is applicable to all cases even in the presence or absence of catalysis (Kasaoka et al., 1986).

The linearized equation for the MVR model can be written as

$$\ln(-[\ln(1-x)]) = \ln a + b \ln \theta \tag{7}$$

A linear plot of $\ln(-[\ln(1-x)])$ versus $\ln \theta$ will give slope $= b$ and intercept $= a$. Since in the gasification process the rate of gasification (defined in terms of the rate constant, $k(x)$, corresponding to conversion, x) varies continuously with time due to continuous structural changes in the carbon matrix, the gasification rate has been expressed as the average rate constant, k:

$$k = \int_0^1 k(x)\,dx \tag{8}$$

The expression for the rate constant, $(k(x)$, as given by Kasaoka et al. (1983), is

$$k(x) = a^{1/b}b[-(\ln(1-x))]^{(b-1)/b} \tag{9}$$

k can be calculated at 50% conversion, i.e., by substituting $x = 0.5$ in eq 9:

$$k = a^{1/b}b(-(\ln 2))^{(b-1)/b} \tag{10}$$

Figures 4 and 5 are the kinetic model plots using the MVR model for the reduction of barite by solid active charcoal under noncatalytic and catalytic conditions, respectively. It is interesting to see that the kinetic conversion–time data of barite reduction by carbon fit the MVR model very nicely in all cases of catalytic and noncatalytic runs. From the slopes and intercepts of the linear plots, model parameters a and b were calculated. By use of the parameter values a and b, the rate constant (k) was obtained for each temperature run. The values of k have been tabulated in Table II. It is observed that both of the catalysts, sodium carbonate and ferric nitrate, have considerable influence in enhancing the value of k and hence the reactivity of coal.

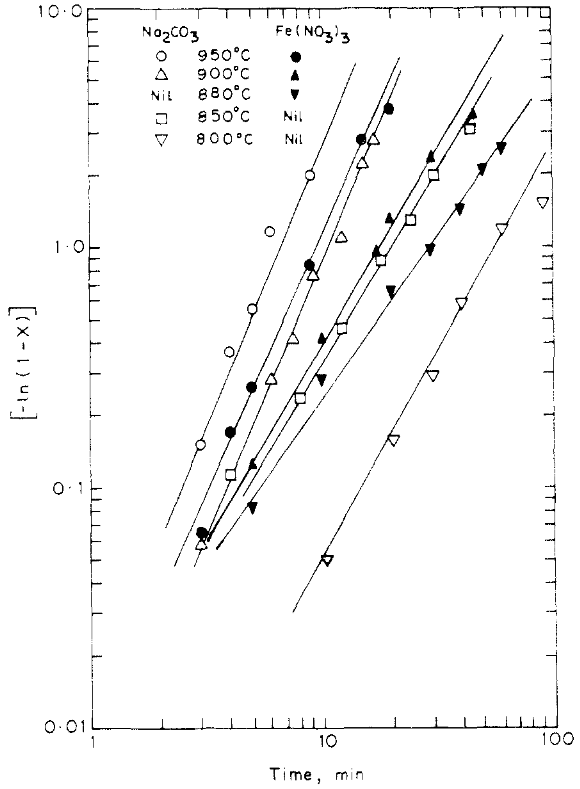

Figure 5. Application of the MVR model to the reduction of barite by active charcoal with 5% catalyst.

Table II. Rate Constant (k) for the Reduction of Barite by Active Charcoal under Catalytic and Noncatalytic Conditions

	k, s^{-1}		
		catalysis due to	
temp, °C	noncatalytic	5% Na_2CO_3	5% $Fe(NO_3)_3$
800		0.45×10^{-3}	
850		1.19×10^{-3}	
880			0.71×10^{-3}
900	0.76×10^{-3}	2.91×10^{-3}	1.29×10^{-3}
950	1.75×10^{-3}	4.84×10^{-3}	3.17×10^{-3}
1000	3.07×10^{-3}		

Arrhenius plots for three typical cases are shown in Figure 6. It is observed that the value of the activation energy for the noncatalytic case was 41.4 kcal/mol, which is close to those obtained for the sodium carbonate catalyzed reaction (41.2 kcal/mol) and the ferric nitrate catalyzed reaction (41.6 kcal/mol), indicating that the mechanism of reduction, in this particular case the mechanism of structural changes in the carbon matrix, is identical in all cases. It is to be noted that during noncatalytic gasification the pore development in the carbon matrix involves typically of micropore development. In the noncatalytic case here, the pore development might be due to micropore development. In the catalytic case, the pore development might be due to micropore development but at an enhanced rate due to presence of cata-

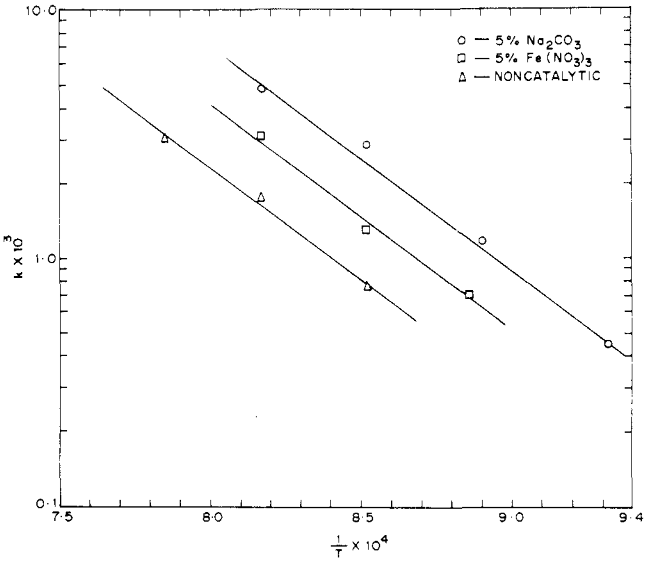

Figure 6. Arrhenius plots for the reduction of barite by active charcoal.

Table III. Arrhenius Parameters for the Reduction of Barite by Active Charcoal under Catalytic and Noncatalytic Conditions

		catalysis due to	
parameter	noncatalytic	5% Na_2CO_3	5% $Fe(NO_3)_3$
E, kcal/mol	41.4	41.2	41.6
A	4.3×10^4	12.0×10^4	8.3×10^4

lyst. Hamilton et al. (1984) showed that in catalytic gasification the rate is proportional to both the number of active sites and the pore development in the carbon matrix where the reaction takes place. However, an increase in the surface area alone is not sufficient to increase the gasification rate; the presence of active sites is more important (Wigmans et al., 1984). The catalysts play a beneficial role of increasing the number of active sites generated in the carbon matrix. This is evident from the fact that the value of the frequency factor, A, which is a measure of the number of active sites, is more in both of the catalytic runs compared to that of the noncatalytic case as shown in Table III. The presence of catalyst ensures a higher number of active sites, being much higher with sodium catalyst since sodium (due to its molten state under the reaction conditions) is prone to disperse in a finely divided state compared to that of ferric nitrate catalyst (McKee, 1981) present in the solid form (metallic Fe). Moreover, the catalyst-to-carbon ratio for Na is three times that of Fe. For Na, it is 2.17 mol of Na/100 g of active charcoal, and for Fe it is 0.69 mol of Fe/100 g of active charcoal.

Conclusions

Reduction of barite by carbon is a typical example of solid–solid reaction proceeding through gaseous intermediate. Since generation of gaseous intermediate CO is the rate-controlling process, incorporation of catalyst to enhance CO generation is also reflected in the enhanced rate of barite reduction. The effect of catalyst has been found to increase the number of active sites for the Boudouard reaction, which is reflected in the enhanced reduction rate of barite correspondingly.

Registry No. $BaSO_4$, 13462-86-7; C, 7440-44-0; CO, 630-08-0; CO_2, 124-38-9; BaS, 21109-95-5; $NaCO_3$, 497-19-8; $Fe(NO_3)_3$, 10421-48-4.

Literature Cited

Cameron, J. H.; Grace, T. M. Kinetic Study of Sulfate Reduction with Carbon. *Ind. Eng. Chem. Fundam.* **1983**, *22*, 486–494.

Doraiswamy, L. K.; Sharma, M. M. *Heterogeneous Reactions Analysis, Examples and Reactor Design*; Wiley: New York, 1984; Vol. I.

Hamilton, T.; David, A. S.; Shadman, F. Variation of Rate During Potassium Catalyzed CO_2 Gasification of Coal Char. *Fuel* **1984**, *63*, 1008–1012.

Kasaoka, S.; Sakata, Y. Fundamental Study on Development of Catalytic Coal Gasification Process. Reports of special project research on energy under grant-in-aid of scientific research; Ministry of Education, Science and Culture: Japan, 1984; pp 239–248.

Kasaoka, S.; Sakata, Y.; Kayano, S. Development of Catalytic Gasification Process for Coal Char, Catalytic Effect and Rate Scheme of Barium Compounds. *Kogaku Kogaku Ronbunshu* **1982**, *8* (1), 51–58.

Kasaoka, S.; Sakata, Y.; Kayano, S.; Masuoka, Y. The Development of Rate Expressions and the Evaluation of Reactivity for Gasification of Various Coal Chars with Steam and Oxygen. *Int. Chem. Eng.* **1983**, *23*, 477–485.

Kasaoka, S.; Sakata, Y.; Tong, C. Kinetic Evaluation of the Reactivity of Various Coals Chars for Gasification with Carbon Dioxide in Comparison with Steam. *Int. Chem. Eng.* **1985**, *25* (1), 161–175.

Kasaoka, S.; Sakata, Y.; Shimada, M. The Sulfur Tolerance of Various Catalysts for the Gasification of Coal Char. *Int. Chem. Eng.* **1986**, *26*, 705–715.

Levenspiel, O. *Chemical Reaction Engineering*; Wiley: New York, 1962.

Lozhkin, A. F.; Pashcenko, V. N.; Povar, F. V. Kinetics of Reduction of Barite by Roasting with Carbon. *J. Appl. Chem. USSR* **1974**, *47* (5), 1031–1034.

McKee, D. Lw. The Catalyzed Gasification Reaction of Carbon. In *Chemistry and Physics of Carbon*; Walker, P. L., Jr., Ed.; Marcel Dekker: New York, 1981; Vol. 16, p 1.

McKetta, J. J., Executive Ed. *Encyclopedia of Chemical Processing and Design*; Marcel Dekker: New York, 1977; Vol. 4.

Pechkovski, V. V.; Ketov, A. N. Study of the Reduction of Barium Sulfate by Carbon Monoxide at High Temperature. *Zh. Prkl. Khim.* **1960**, *33*, 1719–1723.

Pelovski, Y.; Gruchavov, Ir.; Dombalov, I. Barium Sulfate Reduction by Carbon in Presence of Additives. *J. Thermal Anal.* **1987**, *32*, 1743–1745.

Ravdel, A. A.; Novikova, N. A. Reduction of Barite with Carbon. *J. Appl. Chem. USSR* **1963**, *36* (7), 1384–1392.

Shushunov, V. A.; Sadovnikov, G. I.; Andrew, B. Ya. Kinetics of the Reduction of Barium Sulfate. *Zh. Fiz. Khim.* **1954**, *28*, 1472–1478.

Sohn, H. Y.; Szekely, J. Reactions Between Solids Through Gaseous Intermediate I, Reactions Controlled by Chemical Kinetics. *Chem. Eng. Sci.* **1973**, *28*, 1789–1801.

Snell, F. D., Hilton, L., Eds. *Encyclopedia of Industrial Chemical Analysis*; Wiley: New York, 1984; Vol. 6, p 569.

Wen, C. Y. Noncatalytic Heterogeneous Solid Fluid Reaction Models. *Ind. Eng. Chem.* **1968**, *60* (9), 34–54.

Wigmans, T.; Tromp, P.; Moulijn, J. A. On the Interpretation of Reactivity Measurements During Potassium Catalyzed Carbon Gasification Reactions. *Carbon* **1984**, *22* (9), 319–321.

Wynnyckyj, J. R.; Rankin, W. J. An Intrinsic Transport Model for Solid-Solid Reactions Involving a Gaseous Intermediate. *Metall. Trans. B* **1988**, *19B*, 73–81.

Received for review December 12, 1988
Revised manuscript received November 14, 1989
Accepted December 28, 1989